

Divergent resistance at the Dirac point in graphene: evidence for a transition in high magnetic field

Joseph G. Checkelsky, Lu Li and N. P. Ong

Department of Physics, Princeton University, Princeton, NJ 08544, USA

(Dated: August 6, 2008)

We have greatly extended measurements of the Dirac-point resistance R_0 in graphene, using an ultralow-dissipation (<3 fW) technique that avoids self-heating problems. At 0.3 K, $R_0(H)$ is observed to increase a 1000-fold to 40 M Ω in a relatively narrow span of field B . The abruptness of the increase implies that a transition occurs to an insulating, ordered state at large B . Remarkably, R_0 accurately fits a Kosterlitz-Thouless-type correlation length over 3 decades. The results imply a field-induced phase transition to a high-field ordered state that is insulating. The effect of tuning the chemical potential away from the Dirac point is also investigated.

PACS numbers: 73.63.-b, 73.21.-b, 73.43.-f

In graphene, the low energy states display a linear energy-momentum dispersion described by the Dirac Hamiltonian. The observation of the integer quantum Hall (QH) effect by Novoselov *et al.* [1, 2, 3] and Zhang *et al.* [4, 5] has sparked intense interest in this novel 2D (two-dimensional) system. In a strong magnetic field B , the states are quantized into Landau Levels. The Hall conductivity is observed to be accurately quantized as $\sigma_{xy} = (4e^2/h)[n + \frac{1}{2}] = \nu e^2/h$, where e is the electron charge, $2\pi\hbar$ is Planck's constant, and ν the sublevel index. A key question is the nature of the ground state at the Dirac point. In intense B , theory predicts interesting broken-symmetry states driven by exchange and interaction. These are characterized as quantum Hall Ferromagnetism (QHF) [7, 8, 9, 10, 11, 12], or excitonic condensation [13, 14, 15]. These collective states imply the existence of field-induced phase transitions, but the experimental situation is rather unsettled. Moreover, the proposed [12, 16, 17] existence of counter-propagating edge modes at the Dirac point has further enriched the theoretical debate. Is the high-field Dirac point a QH insulator or a QH metal?

Recently, we reported [18] that the resistance at the Dirac point R_0 begins to increase steeply at $B = 10$ -12 T, suggesting a transition to an insulating state. However, the results left open several key questions. Because R_0 increased by only 1-decade (to 0.2 M Ω) [18], we could not establish that the high- B state is truly insulating. Moreover, other explanations – notably carrier localization – could not be excluded. In graphene, the extreme sensitivity to thermal runaway has been highly problematic for researching its high- B ground state [5, 6, 18].

Adopting a technique with ultra-low dissipation, we have overcome this problem. We have measured the divergence in R_0 to values up to 40 M Ω ($\sim 1500 h/e^2$). Remarkably, the divergence is accurately described over 3 decades by the Kosterlitz-Thouless (KT) correlation length. The *singular* nature of the divergence provides strong evidence that a 2D transition to an insulating state occurs when B exceeds a critical field H_c . The systematic variation of H_c with $|V_0|$ (the gate voltage needed to bring the chemical potential μ to the Dirac point) im-

plies a universal phase diagram for graphene. The results exclude localization as the cause of the divergence.

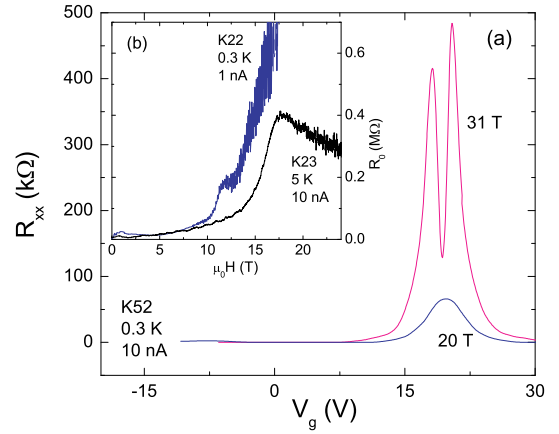


FIG. 1: (color online) Spurious features caused by sample self-heating in graphene. Panel (a) shows a gate-sweep measurement at $T = 0.3$ K of R_{xx} vs. V_g in K52, with I fixed at 10 nA (dc). At $B = 31$ T (red curve), severe self-heating inverts the peak at the Dirac point (R_0 actually exceeds 40 M Ω). Heating effects are less severe in the 20-T curve. Panel (b) displays curves of “ R_0 ” vs. B measured in Samples K22 (at 0.3 K) and K23 (at 5 K) with I fixed at 1 and 10 nA (dc), respectively. When $R_0 > 0.2$ M Ω , self-heating produces the spurious shoulders and broad peaks, whose positions and shapes depend on I .

Near the Dirac point, resistance traces are strongly distorted when the Ohmic heating P exceeds 2 pW for temperatures T below 1 K. As examples, we plot in Fig. 1 resistance traces (with I fixed). In Panel a, the inferred curve of R_{xx} vs. V_g , measured with $B = 31$ T, $I = 10$ nA and $T = 0.3$ K, shows a pronounced dip near the Dirac point caused by self-heating instability (the true R_0 exceeds 10 M Ω). Panel b shows “ R_0 ” vs B measured at fixed I . In the curve for K23 (at 5 K), self-heating reverses the trend of R_0 . The downturn is avoided when I is decreased to 1 nA, but the measured curve (in K22 at 0.3 K) is still greatly suppressed from the true divergent profile.

In our approach, an ac source maintains a fixed voltage amplitude ($40 \mu\text{V}$) across the sample in series with a $100\text{-k}\Omega$ resistor. By phase-sensitive detection of *both* I and the voltage V_{xx} across the sample's voltage leads, we have made 4-probe measurements of R_0 with ultra-low dissipation (P actually decreases from 3 fW at 10 T to 40 aW above 25 T). Moreover, for $T < 1.5 \text{ K}$, the sample is immersed in liquid ^3He so that the electrons in graphene are in direct contact with the bath. The largest reliably-measured R_0 is now $40 \text{ M}\Omega$ (limited by the input impedance of the preamplifier). The new results provide a vastly enlarged view of the interesting region in which R_0 diverges. The sample K52 has an offset voltage ($V_0 = 20 \text{ V}$) much larger than that in K7, the sample investigated in detail in Ref. [18]. In agreement with [18], the field needed to induce the divergence is correspondingly higher.

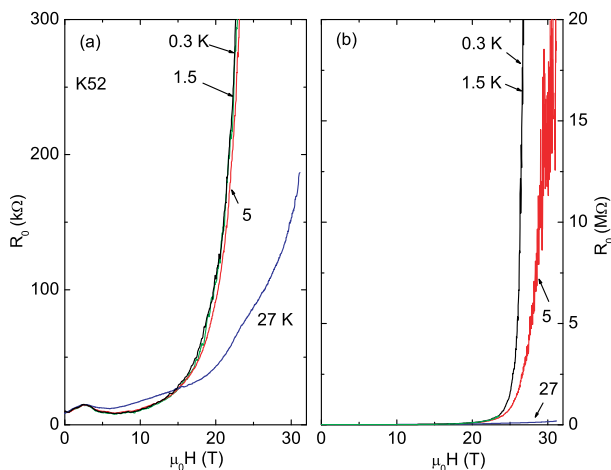


FIG. 2: (color online) Increase of the resistance R_0 at the Dirac point with B at $T = 0.3, 1.5, 5$ and 27 K . Panel a shows the variation up to $300 \text{ k}\Omega$ while b shows the full divergence up to $20 \text{ M}\Omega$. At 27 K , R_0 increases to $190 \text{ k}\Omega$ at 31 T . However, at 0.3 K , R_0 exceeds $40 \text{ M}\Omega$ at 27 T . In Panel b, the curves at 0.3 and 1.5 K (which cannot be distinguished) undergo a 1000-fold increase ($40 \text{ k}\Omega$ to $40 \text{ M}\Omega$) in the interval $17\text{--}27 \text{ T}$. In high B , the 5 K curve deviates significantly from them. The 4-probe voltage-regulated measurement dissipates $\sim 3 \text{ fW}$ at 10 T and 40 aW above 25 T .

Figure 2 shows curves of R_0 vs. B in K52 at the 4 temperatures $T = 0.3, 1.5, 5$ and 27 K at 2 very different resistance scales (up to $300 \text{ k}\Omega$ in Panel a, and to $20 \text{ M}\Omega$ in b). At 27 K , the increase in R_0 is relatively modest (~ 20) between $B = 0$ and 31 T (Panel a). As T decreases to 5 K , the increase steepens sharply, as reported [18] for K7. However, further cooling from 5 to 0.3 K changes the profile only very slightly. In Panel b, the curves at 0.3 and 1.5 K (which cannot be distinguished) show that R_0 diverges to $40 \text{ M}\Omega$, with a slope that continues to accelerate. The nearly vertical increase occurs in the narrow interval $17\text{--}27 \text{ T}$. In contrast to its B dependence, the T dependence of R_0 is quite unusual, as noted previously [18]. If T is lowered with B fixed at 20 T , $R_0(T)$

initially increases, but saturates at $130 \text{ k}\Omega$ for all $T < 4 \text{ K}$. Increasing B lowers the temperature at which saturation occurs. For e.g., if T is lowered with B held at 26 T , R_0 increases very steeply consistent with a large gap Δ opening at the Dirac point. However, below 1.5 K , R_0 saturates at the value $\sim 10 \text{ M}\Omega$. These results confirm that the saturation is intrinsic to the conductance at the Dirac point ($P < 1 \text{ fW}$ at these B values).

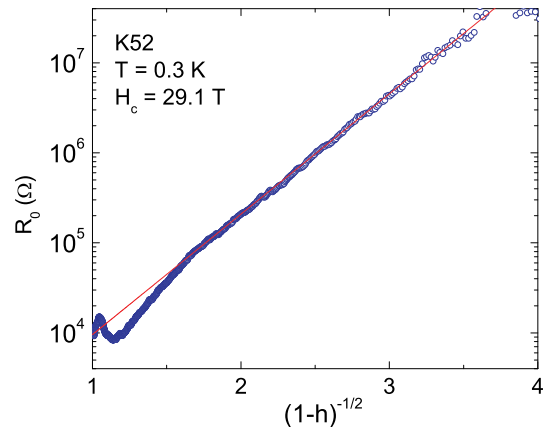


FIG. 3: (color online) Plot of R_0 vs. $1/\sqrt{1-h}$ in K52 at $T = 0.3 \text{ K}$ where $h = H/H_c$. When H_c equals 29.1 T , the high-field data fall on a straight line (curvature is noticeable if H_c is altered by $\pm 0.1 \text{ T}$ from this value). The solid line is the plot of $R_\xi(h) = 440 \exp[2b/\sqrt{1-h}]$, with $b = 1.54$. The data match $R_\xi(h)$ very well over nearly 3 decades in R_0 .

As in Ref. [18], we compare the divergence with that predicted for the Kosterlitz-Thouless (KT) transition. In $2D$ systems described by the XY model, the ordered phase is destroyed at the KT transition by unbinding of pairs of topological excitations (e.g. vortices). As the transition here is induced by varying the applied field H , we replace the reduced temperature t by the reduced field $h = H/H_c$, with H_c the critical field. In the limit $h \rightarrow 1^-$, the KT correlation length ξ diverges as

$$\xi = a \exp[b/\sqrt{1-h}], \quad (1)$$

where a is the lattice parameter and b a number ~ 1 .

The quality of the fit to Eq. 1 is best revealed in a plot of $\log R_0$ vs. the quantity $1/\sqrt{1-h}$ (Fig. 3). Above $\sim 18 \text{ T}$, the data fall on a straight line that extends over nearly 3 decades in R_0 if H_c is chosen to equal 29.1 T . The solid line is the expression $R_\xi(h) = 440 \exp[2b/\sqrt{1-h}]$, with $H_c = 29.1 \text{ T}$ and $b = 1.54$. The value of b is consistent with the KT transition. The 3-decade span places strong constraints that preclude other fits (e.g. power-law divergence). From the quality of the fit, the 3-decade span of R_0 , and the value of b , we find it persuasive that Eq. 1 accurately describes the divergence in R_0 . Hence we infer that, at 0.3 K , we are observing a $2D$ KT-type phase transition to a high-field ordered state that is insulating.

Further insight into the nature of the divergence is obtained by viewing the behavior of the longitudinal resistance R_{xx} vs. V_g in a narrow gate window around the

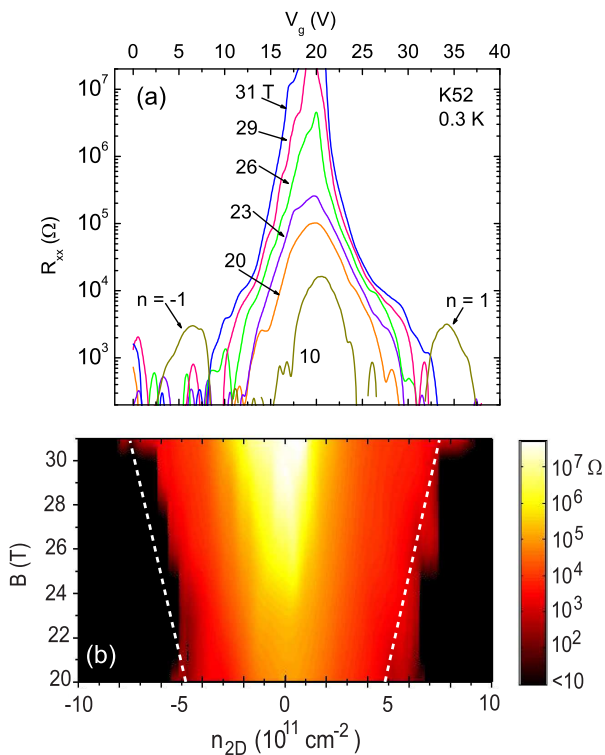


FIG. 4: (color online) Variation of R_{xx} vs. the gate voltage V_g in the interval ($0 < V_g < 38$ V), with B fixed at selected values 10–31 T, and $T = 0.3$ K (Panel a). At $B = 10$ T, the central peak ($n = 0$ LL) is well separated from the LL peaks labelled as $n = \pm 1$. At $B = 20$ T and higher, the $n = \pm 1$ LL’s fall outside the gate window. With increasing B , the central peak increases rapidly and broadens. At the maximum B (31 T), R_{xx} at the Dirac point ($V_g = 20$ V) diverges to values above 40 M Ω . The voltage-regulated technique has poor resolution when R_{xx} falls below 0.3 k Ω . Panel (b) shows the contour plot of $R_{xx}(n_{2D}, B)$ at 0.3 K in the n_{2D} – B plane (color bar of R_{xx} shown on right). The dashed lines trace the sublevel degeneracy $1/2\pi\ell_B^2$. $n_{2D} = CV_g/Ae$ where C and A are the capacitance and area of the device, respectively ($C/A = 1.14 \times 10^{-4}$ Fm $^{-2}$).

Dirac point at fixed B (with T kept at 0.3 K). Figure 4a displays a series of curves of R_{xx} (in log scale) vs. V_g in K52 for fields $10 \leq H \leq 31$ T. At 10 T, R_{xx} displays 3 well-separated peaks corresponding to $n = 0$ LL at 20 V and the $n = \pm 1$ LL’s at 6 and 38 V, respectively. For $H \geq 20$ T, the $n = \pm 1$ levels move out of the gate-voltage window. We focus on the divergent enhancement of the central peak as B increases to 31 T. The key feature is that R_{xx} at the Dirac point ($V_g = 20$ V) rises most rapidly especially for $B > 25$ T.

It is instructive to view R_{xx} (at 0.3 K) as a contour plot in the n_{2D} – B plane where n_{2D} is the 2D density of carriers doped by gating (Fig. 4b). The color bar (right) gives the magnitude of R_{xx} . Interestingly, the steep increase in R_{xx} with B is confined to the region between the dashed lines, which trace the sublevel degeneracy $1/2\pi\ell_B^2$. This suggests that only the states within the lowest sublevels

(on either side of $\nu = 0$) are affected by the opening of the gap Δ . The contours appear to converge to a rounded cusp at $n_{2D} = 0$, but with a curvature that increases rapidly with B . At the largest R_{xx} (white region), the contour resembles a narrow, sharp wedge. The contour pattern suggests that H_c increases very rapidly from the value 29.1 T, as $|n_{2D}|$ deviates from 0.

The physical picture implied by the results is that, at the Dirac point, a field-induced transition to a gapped, insulating state occurs at H_c . The value of H_c is highly sensitive to slight deviations away from exact charge neutrality (Fig. 4). As we decrease H below H_c , the ordered state is unstable to the spontaneous unbinding of (vortex-like) topological excitations which have a mean spacing of ξ (Eq. 1). Because R_0 fits accurately to ξ^2 over 3 decades, we infer that the conductance scales as the density of excitations. Hence the excitations are charged, and they carry the entire current I in the limit $T \rightarrow 0$. As this conduction channel is qualitatively distinct from thermally activated carriers, it may account for the unusual “saturation” behavior of R_0 vs. T [18]. As $T \rightarrow 0$, with H fixed near H_c , the conduction crosses over at 1 K from a steep, thermally activated channel to a T -independent channel carried by the excitations (Fig. 2b).

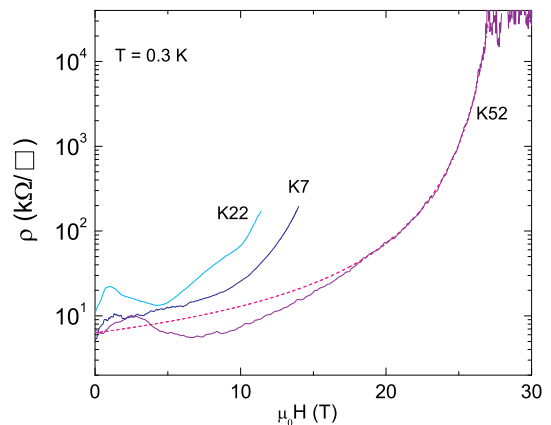


FIG. 5: (color online) Comparison of curves of R_0 (plotted as resistance per square ρ) vs. B in 3 samples K7, K22, and K52 with gate voltage offsets $V_0 = 1, -0.6$ and 20 V, respectively. In samples with smaller $|V_0|$, the divergence in R_0 (plotted in log scale) occurs at a lower B . The dashed curve is the fit of the K52 data to R_ξ .

We next show that the divergence is not consistent with electron localization. As evident from measuring the widths of the peaks of R_{xx} vs. V_g taken in zero B , samples with smallest $|V_0|$ are the least disordered. The electron mobility μ_e decreases from ~ 2.5 to 0.5 T $^{-1}$ as $|V_0|$ increases from 0.5 to 20 V. With this trend in mind, we compare in Fig. 5 the profiles of R_0 vs. B in K52 with K7 and K22 [18]. In Samples K22 and K7 (with $V_0 = -0.6$ and 1 V, respectively), the divergence in R_0 is apparent in relatively low B (below 12 T). By contrast, we must go to much higher fields (> 20 T) in K52. The dashed line is the fit to R_ξ in K52 ($H > 18$ T) described

above.

In the localization scenario, the observed divergence of R_0 in strong field is explained by postulating that B induces localization of the electrons. However, applying this reasoning to the 3 samples in Fig. 5, we would conclude that a modest B is sufficient to trigger the localization in clean samples, but very intense fields are needed in dirtier samples. This implies that disorder and field act in opposition to bring about localization, which is in conflict with physical intuition. In addition, localization induced by B cannot lead to the singular divergence observed in R_0 (Fig. 3). For these reasons, we believe that localization is not a viable explanation for the divergence in R_0 .

In QHF models, Coulomb exchange lifts the 4-fold degeneracy of the $n = 0$ LL at the Dirac point. Spin polarization leads to a spin gap in the bulk at $\nu = 0$. Counter-propagating edge modes (a consequence of lifting of the K - K' degeneracy at the edge) result in a high-field state that is metallic [12, 16, 17]. The present experiment and that in Ref. [18] appear to be in sharp conflict with these predictions. Alicea and Fisher [8] calculate that, if the on-site repulsion energy dominates the Zeeman energy, a gap opens at $\nu = 0$ (edge modes are not considered). Although R_0 is not addressed in Refs. [7, 9, 10], charged skyrmions in graphene are discussed in Ref. [9].

The magnetic-catalysis theory [11, 13, 14, 15] derives from the theoretical finding [19] that the Dirac-point electrons are unstable to the formation of an exciton condensate in a strong B [a solid-state realization of chiral-symmetry breaking in $(2+1)D$]. The order parameter, which measures charge-density differences between the

A and B sublattices, corresponds to a gap at the Dirac point. Khveshchenko [13] predicted that B induces a KT transition to an insulating state with a divergence of the form in Eq. 1. The Kiev-Ontario group [15] recently examined the conditions under which edge modes may be present or absent in the excitonic state. They have uncovered a connection between the excitonic state and QHF models.

Our results – providing direct evidence for a transition at H_c to an insulating state – confirm that interaction effects indeed lead to a broken symmetry state. Using an ultra-low dissipation technique to overcome the self-heating problem, we have measured the divergence in R_0 to 40 M Ω (~ 100 times larger than in all previous reports) while keeping $P < 3$ fW. The divergence in R_0 is shown to follow accurately the KT correlation length over 3 decades as $H \rightarrow H_c^-$. Together, these features imply that the high-field state is truly insulating. Furthermore, the ordered state is approached with a singular divergence in the resistance. An interesting possibility is that the divergence reflects a T -independent conduction channel derived from charged vortex-like excitations. The systematic variation of H_c with V_0 rules out localization as the source of the divergence.

We thank H. A. Fertig, D. V. Khveshchenko and V. A. Miransky for valuable comments, and acknowledge support from NSF-MRSEC under Grant DMR 0213706, and from the Princeton Center for Complex Materials. The experiments were performed at the National High Magnetic Field Laboratory, which is supported by NSF Cooperative Agreement No. DMR-0084173, by the State of Florida, and by the Department of Energy.

-
- [1] K. S. Novoselov *et al.* Science **306**, 666-669 (2004).
 [2] K. S. Novoselov *et al.* Proc. Natl. Acad. Sci. USA **102**, 10451-10453 (2005).
 [3] K. S. Novoselov *et al.* Nature **438**, 197-200 (2005).
 [4] Y. Zhang, J. Tan, H. L. Stormer and P. Kim, Nature **438**, 201-204 (2005).
 [5] Y. Zhang *et al.* Phys. Rev. Lett. **96**, 136806 (2006).
 [6] Z. Jiang, Y. Zhang, H. L. Stormer and P. Kim, Phys. Rev. Lett. **99**, 106802 (2007).
 [7] K. Nomura and A. H. MacDonald, Phys. Rev. Lett. **96**, 256602 (2006).
 [8] J. Alicea and M. P. A. Fisher, Phys. Rev. B **74**, 075422 (2006).
 [9] Kun Yang, S. Das Sarma and A. H. MacDonald, Phys. Rev. B **74**, 075423 (2006).
 [10] M. O. Goerbig, R. Moessner and B. Douçot, Phys. Rev. B **74**, 161407(R) (2006).
 [11] Motohiko Ezawa, J. Phys. Soc. Japan **76**, 094701 (2007).
 [12] D. A. Abanin, P. A. Lee and L. S. Levitov, Phys. Rev. Lett. **96**, 176803 (2006).
 [13] D. V. Khveshchenko, Phys. Rev. Lett. **87**, 206401 (2001); **87**, 246802 (2001).
 [14] V. P. Gusynin, V. A. Miransky, S. G. Sharapov and I. A. Shovkovy, Phys. Rev. B **74**, 195429 (2006).
 [15] V. P. Gusynin, V. A. Miransky, S. G. Sharapov, and I. A. Shovkovy, Europhys. Lett. *in press*, cond-mat arXiv:0801.0708.
 [16] H. A. Fertig and L. Brey, Phys. Rev. Lett. **97**, 116805 (2006).
 [17] D. A. Abanin *et al.* Phys. Rev. Lett. **98**, 196806 (2007).
 [18] Joseph G. Checkelsky, Lu Li, and N. P. Ong, Phys. Rev. Lett. **100**, 206801 (2008).
 [19] V. P. Gusynin, V. A. Miransky, and I. A. Shovkovy, Phys. Rev. Lett. **73**, 3499 (1994); Phys. Rev. D **52**, 4718 (1995).